Dissociative Electron Transfer, Substitution, and Borderline Mechanisms in Reactions of Ketyl Radical Anions. Differences and Difficulties in Their Reaction Paths

Sason Shaik,*,† David Danovich,† G. Narahari Sastry,‡ Philippe Y. Ayala,§ and H. Bernhard Schlegel*,§

Contribution from the Department of Organic Chemistry and the Lise Meitner-Minerva Center of Computational Quantum Chemistry, The Hebrew University, Jerusalem 91904, Israel, Institute of Physical Chemistry, University of Fribourg, Perolles, CH-1700 Fribourg, Switzerland, and Department of Chemistry, Wayne State University, Michigan 48202

Received April 7, 1997. Revised Manuscript Received July 10, 1997[⊗]

Abstract: Computational studies on ketyl anion radicals with methyl chloride and on ω-chloroalkanal radical anions, $Cl(CH_2)_nC(H)O^{-\bullet}$ ($n = 2$, 3), find competing mechanisms: a dissociative electron transfer (ET) mechanism and a substitution (SUB(C)) mechanism leading to a C-alkylation product. $H(CN)C{=}O^{-\bullet}/CH_3Cl$ proceeds unequivocally via the SUB(C) mechanism, and ω-chloroalkanal radical anions proceed by the ET mechanism, but the interpretation of the mechanism for $H_2C{=}O^{-\bullet}/CH_3Cl$ depends on the coordinate system used to explore the path. The steepest descent path in Z-matrix internal coordinates leads to the ET product at both the ROHF/6-31G* and UHF/6-31G* levels. The mass-weighted path leads to the ET product on the restricted open-shell Hartree−Fock (ROHF) surface but to the SUB(C) product on the unrestricted Hartree−Fock (UHF) surface. A valley−ridge inflection point heading in the direction of ET products was located on the mass-weighted UHF path, indicating that the potential energy surface branches toward ET products. Closer examination of the two-dimensional portion of the surface shows that the potential energy surface for this reaction descends from the transition state to a broad saddle point region and branches into two valleys: one leading to the ET product and the other to the SUB(C) product. The ridge and saddle point region on the UHF surface are at lower energy and longer C−C and C−Cl bond lengths than on the ROHF surface, allowing the UHF mass-weighted reaction path to traverse the ridge into the SUB(C) valley. On the ROHF surface as the path descends from the transition state, the $H_2C{=}O^{-\bullet}$ moiety continues to approach the methyl chloride while the C−Cl bond lengthens, but then recoils to give the ET products. Cross-sections of the surface calculated at the UQCISD(T)/6-31G* level resemble the UHF cross-sections, indicating that the branching of the potential surface into two mechanisms is expected at this level, too. Thus, whereas from inspection of the surface in internal coordinates, the $OCH_2C{-}CH_3{-}Cl^-$ transition state connects to the ET product, the mass-weighted path can cross the broad and shallow ridge and bifurcate thereafter to ET and SUB(C) products. Our study reveals a scenario where a group of isostructural transition states define a mechanistic family consisting of substitution, electron transfer, and borderline situations. Molecular dynamics studies may be necessary to explore the borderline situations.

Introduction

Recently two of us have reported computational studies of a group of reactions between ketyl radical anions and alkyl halides, as well as those of intramolecular processes of ω-chloroalkanal radical anions, $Cl(CH_2)_nC(H)O^{-\bullet}$ ($n = 2$,3), Scheme 1.[1−3] The reaction group of $Y(H)C{=}O^{-\bullet}/CH_3X$ was found to exhibit a mutually exclusive competition between a dissociative electron transfer (ET) mechanism, **2a**, and a substitution (SUB(C)) process which leads to a C-alkylation product, **3a**. For example, the reaction of formaldehyde radical anion with methyl chloride leads to dissociative ET, while the cyanoformaldehyde radical anion proceeds to SUB(C). The transition states (TS) for both reactions have the general structure of **1a** in Scheme 1, with partial C−C bonding between the reactants. The intermolecular distance between the reactant pair (R_{CC}) delineates the mechanistic changeover from ET to SUB(C):[2] the looser transition states (with $R_{CC} \geq 2.5$ Å) lead to ET products while the tighter ones (with $R_{CC} \leq 2.4$Å) lead to SUB(C).[1,4] In contrast, no SUB(C)-TS could be located for the intramolecular reactions which were found to proceed exclusively to ET products,[3] via TS structure type **1b**, in accord with the experimental results reported[5] for ω-haloalkyl phenyl ketyl radical anions which gave ET but no C-alkylation products. Thus, a case has been made for isostructural TS which possess partial C−C bonding and which lead to competing ET and SUB(C) mechanisms.

The discussion of "bonded" ET-TS has, of course, not gone without controversy. Recently, Bertran et al.[6] as well as Sastry and Shaik[7] showed, for the $H_2C{=}O^{-\bullet}/CH_3Cl$ system, that the interpretation of the $OH_2C{\cdots}CH_3{\cdots}Cl^-$ structure as either an ET-TS or a SUB(C)-TS depends on the wave function (ROHF vs UHF) as well as on the coordinate system one uses

† The Hebrew University.
‡ University of Fribourg.
§ Wayne State University.
⊗ Abstract published in *Advance ACS Abstracts,* September 1, 1997.

(1) Sastry, G. N.; Shaik, S. *J. Am. Chem. Soc.* **1995**, *117*, 3290.
(2) Sastry, G. N.; Danovich, D.; Shaik, S. *Angew. Chem., Int. Ed. Engl.* **1996**, *35*, 1098.
(3) Sastry, G. N.; Reddy, A. C.; Shaik, S. *Angew. Chem., Int. Ed. Engl.* **1995**, *34*, 1495.
(4) The absolute R_{CC} value at which the mechanistic changeover occurs, of course, depends on the choice of the method. But at the HF level (whether UHF or ROHF), the mechanistic changeover seems to occur over this short boundary.
(5) Kimura, N.; Takamuku, S. *J. Am. Chem. Soc.* **1994**, *116*, 4087; *Bull. Chem. Soc. Jpn.* **1991**, *64*, 2433.
(6) Bertran, J.; Gallardo, I.; Moreno, M.; Savéant, J.-M. *J. Am. Chem. Soc.* **1996**, *118*, 5737.
(7) Sastry, G. N.; Shaik, S. *J. Phys. Chem.* **1996**, *100*, 12241.

S0002-7863(97)01105-0 CCC: $14.00

Scheme 1

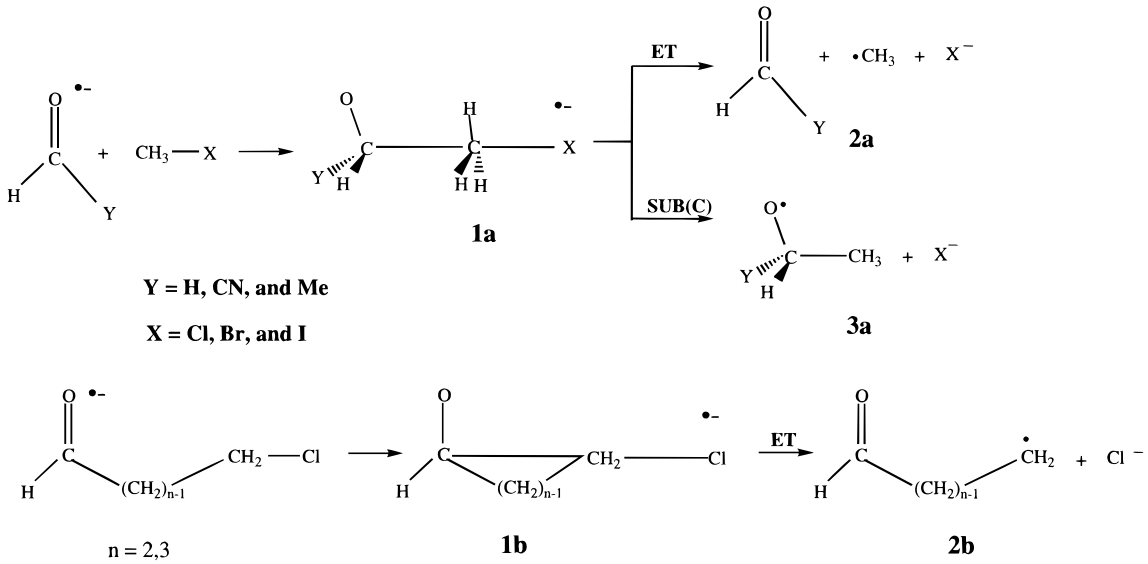

to follow the path. This ambiguity prompted us to take a more extensive study of the controversial reaction and to calculate a multidimensional potential energy surface which might reveal the cause for the behavior of this system. Such a study, which probes the mechanism by which a bonded ET-TS undergoes a C−C recoil to give dissociated ET products, whereas a similar-looking SUB(C)-TS collapses to SUB(C) products, may be fundamentally important for understanding the mechanistic dichotomy often discussed in the literature for ET and related bond-forming reactions.[8] Furthermore, in reactions between arene anion radicals and neutrals, it is the recoil mechanism that will differentiate a bonded-ET from a bond-forming process. Thus, finding a mechanism by which a bonded-ET transition state loses its bonding en route to ET products is a question of general importance and has bearing on all innersphere ET reactivity.[8e,j]

Methodology

General Computational Considerations: Elucidation of Reaction Mechanisms. A reaction mechanism can be explored computationally by finding the steepest descent path that connects the transition state to reactants and to products. The particular route that a steepest descent path takes depends on the coordinate system, e.g., Cartesian coordinates, various definitions of internal coordinates, or mass-weighted (MW) coordinates. When mass-weighted coordinates are used, the resulting path is also called the intrinsic reaction coordinate (IRC).[9] If the potential energy surface is characterized by a well-defined valley connecting the reactants, transition state, and products, then following the steepest descent path in any coordinate system (with or without mass weighting) will yield the same general description of the reaction mechanism. However, if the potential energy surface has wide slopes, broad flat areas, or branching valleys, then different coordinate systems (and different levels of theory) can lead to quite different steepest descent paths. Ultimately, the interpretation of a reaction mechanism on difficult potential energy surfaces may have to rely on reaction dynamics rather than reaction paths.

With these considerations in mind, let us review the path-following behavior exhibited[6,7] in the reaction of formaldehyde anion radical with methyl chloride. With spin-restricted open-shell Hartree−Fock (ROHF) theory, path-following in various mass-weighted and non-mass-weighted coordinate systems shows that the transition state for formaldehyde radical anion and methyl chloride (structure **1a**, Scheme 1) leads to dissociated ET products, **2a**.[1,2,7] In contrast, with spin-unrestricted Hartree−Fock (UHF) or Møller−Plessett second-order perturbation (UMP2) theories, path-following with mass-weighted internal coordinates leads to SUB(C) products, while path-following in non-mass-weighted internal coordinates from the same transition state leads to ET products at all levels studied.[7]

These contrasting results are disconcerting and create confusion about the mechanisms of this group of reactions. To elucidate the source of these difficulties, we have undertaken a comparative study of four systems: $H(CN)C{=}O^{-\bullet}/CH_3Cl$, $Cl(CH_2)_nC(H)O^{-\bullet}$ (n = 2, 3), and $H_2C{=}O^{-\bullet}/CH_3Cl$. For the first three systems, reaction path-following was sufficient to characterize the mechanism; for the last system, two-dimensional potential energy surface was needed to interpret the behavior of the reaction path-following.

Technical Details: All of the calculations were performed using the Gaussian suite of programs.[10] Transition state geometries, reaction paths, projected frequencies, and potential energy surfaces were obtained at the UHF/6-31G* and ROHF/6-31G* levels. Higher level calculations for $H_2C{=}O^{-\bullet} + CH_3Cl$ are discussed in ref 7, and not reviewed here, due to the identity of the qualitative features at all levels. Some additional points on the potential energy surface were calculated by quadratic configuration interaction, UQCISD(T)/6-31G*,[11] to assess the effects of electron correlation and spin contamination.

Reaction paths were followed using the second-order Gonzalez−Schlegel algorithm[12] at the UHF/6-31G* and ROHF/6-31G* levels. Steepest descent paths in Z-matrix internal coordinates without mass weighting are designated Z-Int, and in mass-weighted Z-matrix internal coordinates (which is equivalent to mass-weighted Cartesian coordi-

(8) (a) Pross, A. *Acc. Chem. Res.* **1985**, *18*, 212. (b) Kochi, J. K. *Angew. Chem., Int. Ed. Engl.* **1988**, *27*, 1227. (c) Eberson, L. *New. J. Chem.* **1992**, *16*, 151. (d) Lund. H.; Daasberg, K.; Lund. T.; Pedersen, S. U. *Acc. Chem. Res.* **1995**, *28*, 313. (e) The terminology inner sphere is used to emphasize that the reactant moieties maintain bonding in the ET-TS. See, Eberson, L.; Shaik, S. S. *J. Am. Chem. Soc.*, **1990**, *112*, 4484. (f) Savéant, J. -M. *Adv. Phys. Org. Chem.* **1990**, *26*, 1. (g) Garst, J. F.; Smith, C. D. *J. Am. Chem. Soc.* **1976**, *98*, 1520. Garst, J. F. *Acc. Chem. Res.* **1971**, *4*, 400. (h) Bilkis, I. I., Selivanov, B. A.; Shteingarts, V. D. *Res. Chem. Intermed.* **1993**, *19*, 463. (i) Honda, E.; Tokuda, M.; Yoshida, H.; Ogasawara, M. *Bull. Chem. Soc. Jpn.* **1987**, *60*, 851. (j) Eberson, L. *Electron Transfer Reactions in Organic Chemistry*; Springer Verlag: Heidelberg, 1987. (k) Chanon, M. *Bull. Chim. Soc. Fr.* **1982**, *Part II*, 197.

(9) Fukui, K. *Acc. Chem. Res.* **1981**, *14*, 363.

(10) Frisch, M. J.; Trucks, G. W.; Schlegel, H. B.; Gill, P. M. W.; Johnson, B. G.; Robb, M. A.; Cheeseman, J. R.; Keith, T.; Petersson, G. A.; Montgomery, J. A.; Raghavachari, K.; Al-Laham, M. A.; Zakrzewski, V. G.; Ortiz, J. V.; Foresman, J. B.; Cioslowski, J.; Stefanov, B. B.; Nanayakkara, A.; Challacombe, M.; Peng, C. Y.; Ayala, P. Y.; Chen, W.; Wong, M. W.; Andres, J. L.; Replogle, E. S.; Gomperts, R.; Martin, R. L.; Fox, D. J.; Binkley, J. S.; Defrees, D. J.; Baker, J.; Stewart, J. P.; Head-Gordon, M.; Gonzalez, C.; Pople, J. A.; Gaussian 94; Gaussian, Inc.: Pittsburgh, PA, 1995.

(11) Pople, J. A.; Head-Gordon, M.; Raghavachari, K. *J. Chem. Phys.* **1987**, *87*, 5968.

(12) Gonzalez, C.; Schlegel, H. B. *J. Chem. Phys.* **1989**, *90*, 2154; *J. Phys. Chem.* **1990**, *94*, 5523.

nates) are designated MW or IRC (for intrinsic reaction coordinate). It should be mentioned that the IRC converges slowly and one needs many steps. For the intramolecular reaction of $Cl(CH_2)_nC(H)O^{-\bullet}$ ($n = 3$), the IRC was difficult to follow, requiring a smaller step size and more steps (0.05 amu$^{1/2}$ a_0 and 100 steps).

Projected Hessians or projected frequencies (where motion along the reaction path has been projected out) can be used to characterize the normal modes *perpendicular the path*.[13] The projection, which has to be carried out at each of the IRC(MW) points, characterizes the nature of the path at a given point. If all of the eigenvalues of the projected Hessian are positive or all of the projected frequencies are real, then the path is in a valley (the smaller the lowest eigenvalues or projected frequencies, the broader the valley). If one of the eigenvalues is negative or one of the projected frequencies is imaginary, then the path is on a ridge. The point at which a valley changes to a ridge is called a valley−ridge inflection (VRI) point[14] and is characterized by a zero eigenvalue of the projected Hessian or a zero projected frequency. VRI points were found by following the MW path with a step size of 0.001 amu$^{1/2}$ a_0, monitoring the projected frequencies and interpolating to find the structure with a zero projected frequency. Because of the nature of a steepest descent path, it remains on the ridge for a considerable distance beyond the VRI point before descending into one of the valleys or reaching a stationary point.[14c] Note that the presence of imaginary projected frequencies is merely a sign that the path is on a ridge, but this is not a condition sufficient to require the surface to branch into separate valleys (since they can merge again into a single valley further down the slope of the potential energy surface).

The full 21-dimensional potential energy surface for $H_2C{=}O^{-\bullet} + CH_3Cl$ is rather difficult to visualize. To examine the portion of the surface related to the reaction, we have constructed a two-dimensional subspace containing the mass-weighted and non-mass-weighted reaction paths. Approximately 250 additional geometries were obtained by linear interpolation of suitable structures on the mass-weighted and non-mass-weighted UHF reaction paths. Energies for these structures were calculated at both the UHF and ROHF levels. Mathematica[15] was used to fit a two-dimensional fifth order polynomial in the C−C and C−Cl bond lengths to the reaction paths and ca. 250 additional points for the UHF surface and likewise for the ROHF surface. On a rectilinear plot of the surface in terms of the C−C and C−Cl bond lengths, the Z-Int path is the line of steepest descent from the transition state. The MW path or IRC is the steepest descent line in mass-weighted coordinates. For a simple triatomic reaction, A + BC → AB + C, plotting the mass-weighted surface simply involves scaling the axes and skewing them to an angle smaller than 90°.[16] The scale factors and angle can be computed from the masses of A−C. For the $H_2C{=}O^{-\bullet} + CH_3Cl$ reaction, a good approximation to the mass weighting can be obtained by taking $H_2C{=}O^{-\bullet}$ as fragment A, CH_3 as B, and Cl as C. The scale factor of the C−Cl axis relative to the C−C axis is 0.98 and the angle between the axes is 47°. When plotted with these scaled and skewed axes, a steepest descent line on the fitted surface approximates a MW path or IRC.

Results and Discussion

Scheme 2 shows the TS structures for the four reactions, optimized at the UHF/6-31G* level of theory.[1−3] Corresponding ROHF/6-31G* structures which are very close can be found in refs 2 and 7. It is apparent, therefore, that all four reactions possess isostructural TS structures, which nevertheless exhibit different mechanistic behavior. Since only **4b** leads to an ambiguous assignment, this reaction was investigated in detail at both the ROHF and UHF levels; for **4a**, **4c**, and **4d**, we focus on the UHF results.

Scheme 2

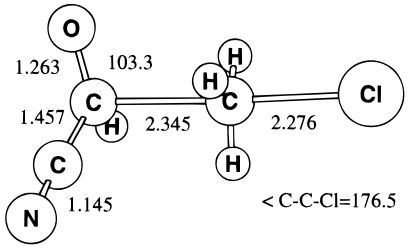

4a, SUB(C)-TS

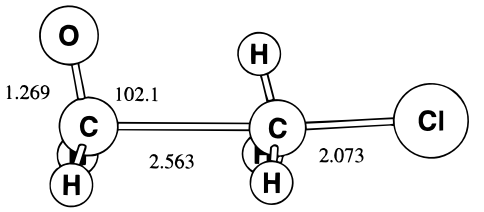

4b, ET-TS

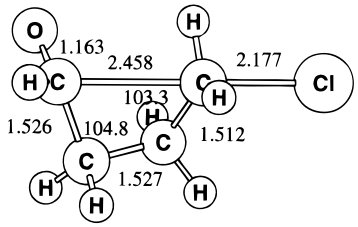

4c, ET-TS

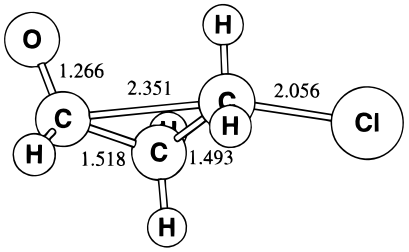

4d, ET-TS

H(CN)CO$^{\bullet-}$ + CH$_3$Cl Energetics. Figure 1 shows the UHF potential energy profile of the SUB(C) mechanism leading to cluster $C_{SUB(C)}$ and also the successive step which involves C−C bond breaking and leads to the cluster of ET products, C_{ET}. The projected frequencies are positive at all points along the MW path. This is a standard behavior of a reaction path which passes through a simple valley. Thus, **4a** is a classical SUB-(C) transition state, and the reaction path from **4a** leads to SUB-(C) products (Figure 1). The values of $\langle S^2 \rangle$ for transition state is 0.79 and rises to a maximum of 0.83 along the reaction path. This small variation suggests that spin contamination does not cause significant distortion of the potential energy surface for this reaction. The subsequent transition structure on the path is for radical attack (R_{AT}-TS, Figure 1), which connects the SUB(C) cluster and the ET cluster in an endothermic process.

Cl(CH$_2$)$_n$C(H)O$^{-\bullet}$ Energetics. Figure 2 shows the UHF energies for the intramolecular process for $n = 3$. A similar

(13) The projected frequencies calculated by Gaussian 94 and earlier programs are valid only for MW or IRC paths since the projection is applied to the mass-weighted Hessian.

(14) (a) Valtazanos, P.; Ruedenberg, K. *Theor. Chim. Acta.* **1986**, *69*, 281. (b) Hoffmann, D. K.; Nord, R. S.; Ruedenberg, K. *Theor. Chim. Acta.* **1986**, *69*, 265. (c) Schlegel, H. B. *J. Chem. Soc., Faraday Trans.* **1994**, *90*, 1569. See also the general discussion following this paper. (d) Garrett, B. G.; Truhlar, D. G.; Wagner, A. F.; Dunning, T. H., Jr. *J. Chem. Phys.* **1983**, *78*, 4400. Natanson, G. A.; Garrett, B. C.; Truong, T. N.; Joseph, T.; Truhlar, D. G. *J. Chem. Phys.* **1991**, *94*, 7875. (e) Baker, J.; Gill, P. M. W. *J. Comput. Chem.* **1988**, *9*, 465.

(15) Wolfram, S. *Mathematica*; Addison-Wesley: Reading, MA, 1991.

(16) Steinfeld, J. I.; Francisco, J. S.; Hase, W. L. *Chemical Kinetics and Dynamics*; Prentice Hall: Englewood Cliffs, NJ, 1989.

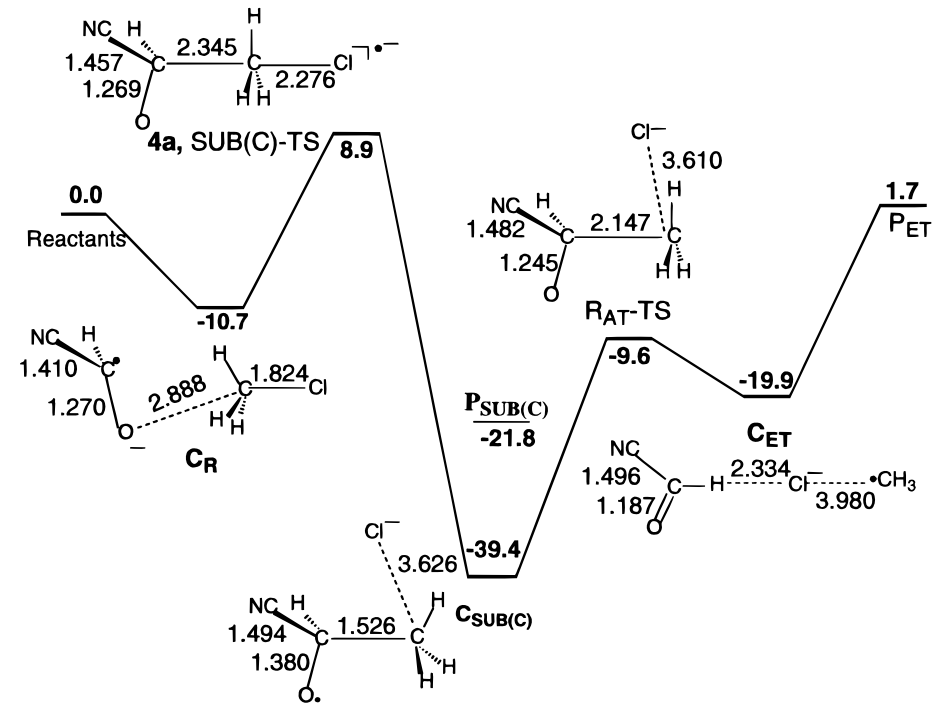

Figure 1. The UHF/6-31G* energy profile of $H(CN)CO^{-\bullet}$ + CH_3Cl. Relative energies are given in kcal/mol, distances are in angstroms, and angles are in degrees. C_R, $C_{SUB(C)}$, and C_{ET} are the reactant, SUB(C), and ET clusters, respectively. R_{AT}-TS is the radical attack TS, and P_{ET} is the ET product.

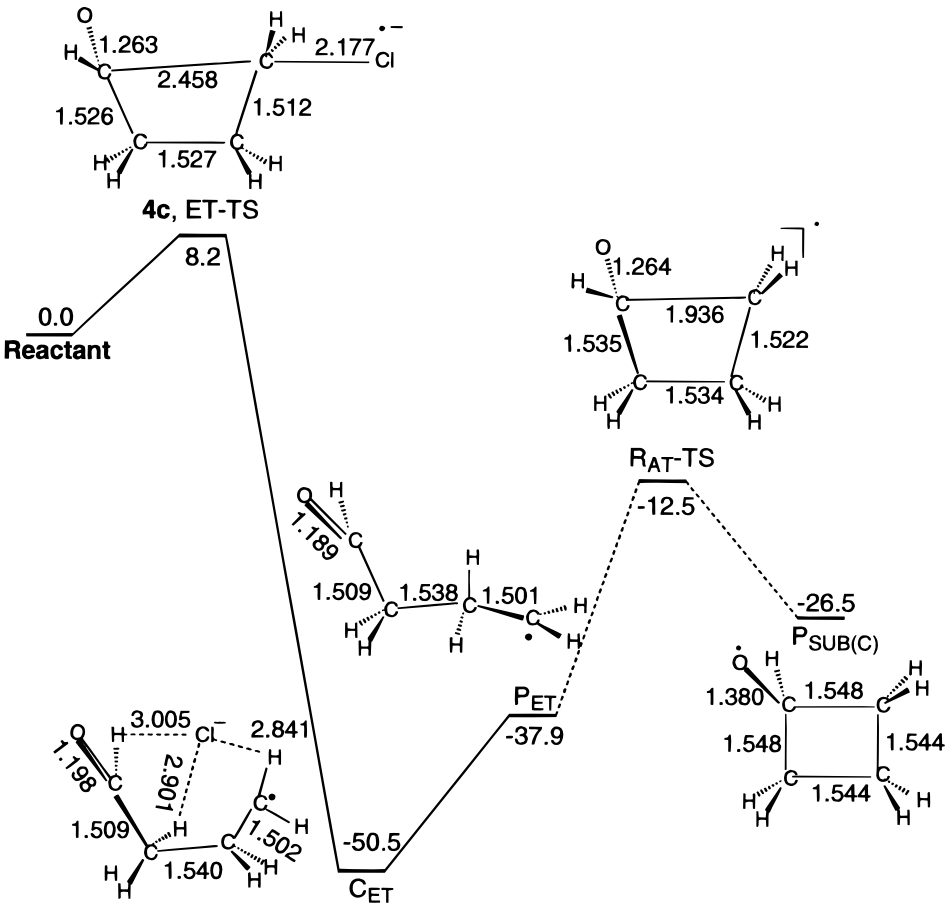

Figure 2. The UHF/6-31G* energy profile of $Cl(CH_2)_3C(H)O^{-\bullet}$. Relative energies are given in kcal/mol, distances are in angstroms, and angles are in degrees. The labels of the species are as in Figure 1.

figure applies to the system with $n = 2$ (not shown). For each of the two molecules, both Z-Int and MW paths lead the TS, **4c** and **4d**, to the cluster of the ET products, C_{ET}. In both cases, the C−C distance initially decreases and then recoils getting progressively larger toward the ET product. For both molecules, the MW path has imaginary frequencies in the projected Hessian. For $n = 2$, the imaginary projected frequency is quite complex, and may best be described as a mode which involves

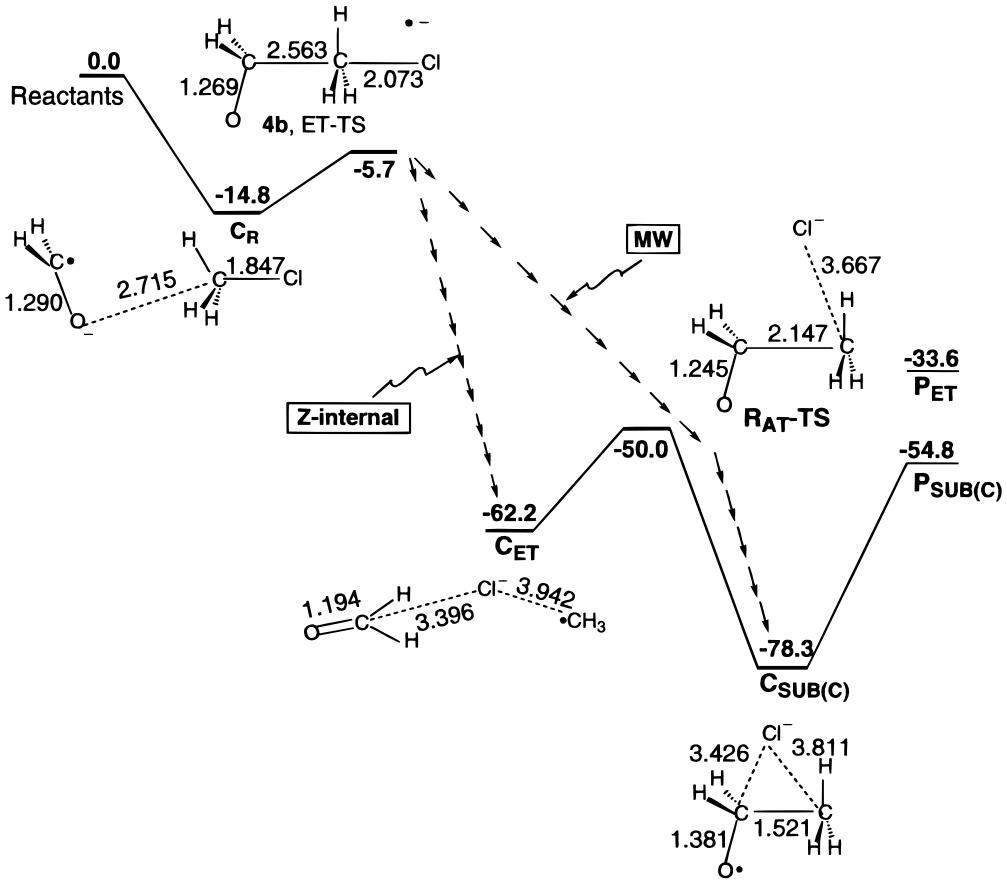

Figure 3. The UHF/6-31G* energy profile of $H_2CO^{-\bullet} + CH_3Cl$. Relative energies are given in kcal/mol, distances are in angstroms, and angles are in degrees. The labels of the species are as in Figure 1.

rotations of the CH_2 and CHO groups. For $n = 3$, there are two imaginary projected frequencies, again of complex character. Near the transition state, one of the projected frequencies has some character of C−C bond making (even though the orbitals are not clearly aligned for bonding), while the other is a mixed stretching mode of the backbone C−C bonds and rocking of some of the hydrogens. The first imaginary frequency disappears near the point where the C−C bond recoils to lead to ET products. These features indicate that the MW path starts on a ridge and then desends to the ET valley. Thus, both path-following methods give an unequivocal assignment that **4c** and **4d** are ET-TS. The ET mechanisms of the $Cl(CH_2)_nC(H)O^{-\bullet}$ systems are in good accord with experimental results of the analogous $X(CH_2)_nC(Ar)O^{-\bullet}$ (X = I, Br, Cl; Ar = aryl) systems,[5] which participate in an ET mechanism but exhibit no SUB(C) reactivity.

For both the $n = 2$ and 3 cases, the subsequent process of radical coupling, which generates the SUB(C) product, was studied without the presence of Cl^-, a mere spectator species,[1,7] and was found to be uphill and to possess a significant barrier, reflecting the strain of the small rings. Figure 2 shows this process for $n = 3$.

$H_2CO^{-\bullet} + CH_3Cl$ Energetics. Figure 3 depicts the UHF potential energy profile for $H_2C{=}O^{-\bullet} + CH_3Cl$. The Z-Int path leads to the cluster of the ET products, C_{ET}, whereas the MW path leads to the SUB(C) cluster, $C_{SUB(C)}$. The ET and SUB(C) clusters are connected by a radical attack transition state, R_{AT}-TS. The MW path was found to move on a ridge and to have *a VRI point which exits toward the ET products*. Thus, along the MW path, two of the projected frequencies become imaginary, indicating that the path is on a ridge. As shown in Figure 4, one mode, a, clearly leads to the ET products while

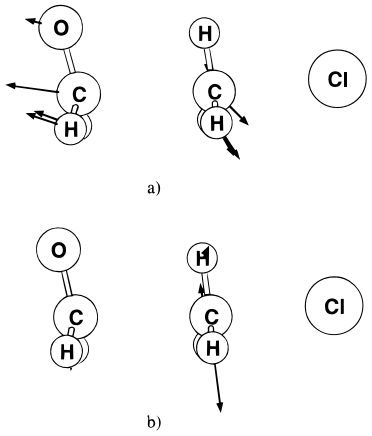

Figure 4. Normal modes of two imaginary projected frequencies along the MW path on the UHF surface for $H_2CO^{-\bullet} + CH_3Cl$. Mode a leads to ET.

Scheme 3

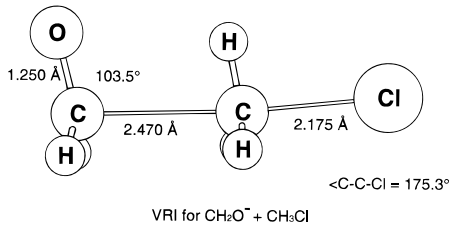

the other mode, b, is a simple methyl rotation. Scheme 3 shows the structure of the VRI point related to the ET/SUB(C) branching. The VRI is close to the TS but is not itself a stationary point. The MW path remains on this ridge for a

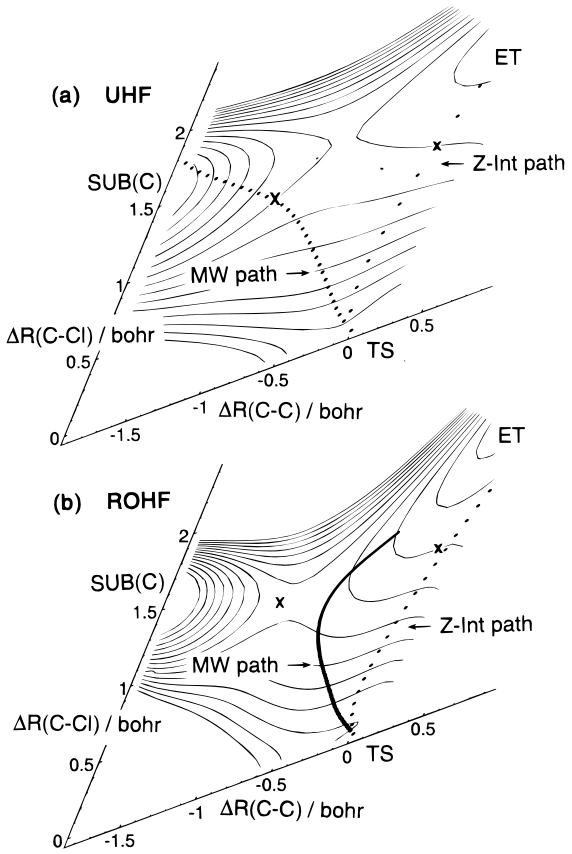

Figure 5. Contour plot of a portion of the mass-weighted potential energy surface containing the Z-Int and MW paths for $H_2CO^{-\bullet} + CH_3$-Cl computed at the (a) UHF and (b) ROHF levels of theory (contour lines at 5 kcal/mol intervals).

considerable distance beyond the VRI point. For the ROHF calculations, the path eventually descends from the ridge into the ET valley; for the UHF calculations, it descends into the SUB(C) valley. The values of $\langle S^2 \rangle$ for the transition state on the UHF surface is 0.76 and rises to a maximum of 0.88 along the reaction path, indicating that spin contamination could distort the potential energy surface.

Potential Energy Surface along the Reaction Paths for $H_2CO^{-\bullet} + CH_3Cl$. To understand the different behavior of the MW and Z-Int paths for the ROHF and UHF calculations, we have fitted a model surface to a two-dimensional subspace of the potential energy surface that contains the reaction paths. Contour plots of the relevant portions of the UHF and ROHF model surfaces (mass weighted) are shown in Figure 5a and b, respectively, along with the Z-Int and MW reaction paths. The surfaces are strikingly similar in their features. Both have two valleys separated by a shallow ridge: one valley stretches from the TS toward the ET product and, across the ridge, a second valley goes to SUB(C) products. In the ROHF surface, the ridge is a little higher and at shorter C−C and C−Cl bond lengths.

Let us now discuss the path-following on these surface. Both potential energy surfaces descend rapidly from the transition state to a broad saddle region, corresponding to the radical attack TS (see R_{AT}-TS in Figure 3) which connects the valleys of the ET and SUB(C) products. The Z-Int paths on both surfaces proceed downhill in the ET valley, to the long C−C side of the saddle region, and then descend to the ET products. In the MW path, the lighter CH_3 group moves more than the heavier H_2-CO and Cl^- groups; this motion involves the shortening of the C−C bond and the lengthening of the C−Cl bond and leads the MW path to the ridge region. On the UHF surface, the

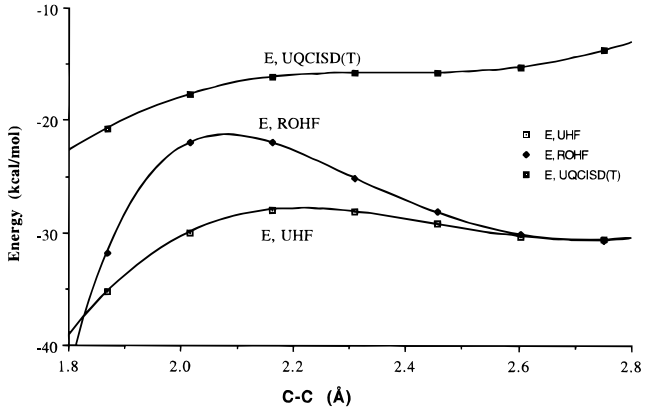

Figure 6. Cross-section of the potential energy surface in Figure 5 with a C−Cl bond length near 2.7 Å (passing through the points marked with X's) computed at the ROHF, UHF, and UQCISD(T) levels of theory.

MW path crosses the ridge and heads toward the short C−C side of the R_{AT}-TS saddle region and descends into the SUB-(C) valley. On the ROHF surface, the MW path starts in the same direction; however, the R_{AT}-TS saddle region lies higher in energy and at shorter C−C and C−Cl bond lengths. Consequently, the MW path bounces back off the ridge and descends on the ET side of the region, ending at the well of the ET products.

The differences between the UHF and ROHF surfaces are more apparent in cross-sections of the potential energy surface, as shown in Figure 6. The ROHF surface is distinctly sloped toward the ET product and has a significant ridge which deflects the path away from the SUB(C) products. In contrast, the UHF path, although sloping gently toward the ET, has a very shallow ridge to cross en route to the SUB(C) product. Thus, while the ROHF surface clearly favors an ET assignment for the reaction, the UHF surfaces favor a situation where the ET-TS can lead to two products if sufficient kinetic energy is available to move from the ET valley across the ridge.

Since it is unclear whether the ROHF or UHF surface is a better approximation, the cross-section was also calculated at the UQCISD(T)/6-31G* level, providing a better treatment of electron correlation than Møller−Plesset perturbation theory and less susceptibility to spin contamination effects.[17] It is seen, from Figure 6, that the UQCISD(T) cross-section is more similar to the one obtained by UHF, with little or no barrier separating the two paths in this cross-section. *Thus, while inspection of the surface in internal coordinates qualifies the $OH_2C-CH_3-Cl^-$ structure as an ET-TS because it is connected to the ET product via a continuously descending valley, the nature of the MW path and the very shallow ridge separating the ET and SUB(C) pathways indicate that whenever the reaction system enters the flat ridge region the path may bifurcate thereafter to the ET and SUB(C) products*. The nature of the branching valleys of the potential energy surface for this reaction suggests that molecular dynamics and statistical considerations may ultimately be needed to interpret the mechanism(s) of this model system. We mention that, experimentally, intermolecular reactions of ketyl radical anions and alkyl halide lead mostly to ET and O-alkylation but participate rarely in the SUB(C) mechanism.[8g−i] Nevertheless, the possibility of an ET-TS with a branching toward SUB(C), and vice versa, cannot be dismissed.

A Recoil Mechanism for Bonded ET-TS. The departure of Cl^- is common to the SUB(C) and ET mechanisms, and it

(17) Chen, W.; Schlegel, H. B. *J. Chem. Phys.* **1994**, *101*, 5957.

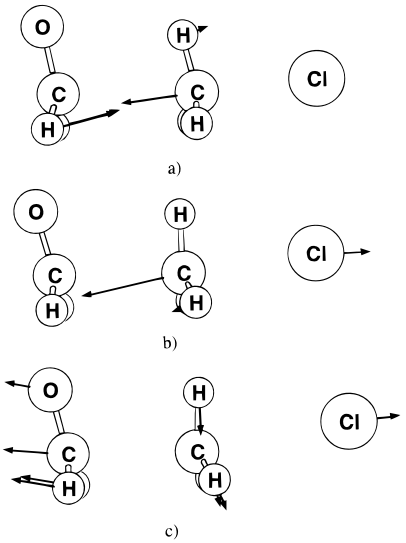

Figure 7. Reaction vector along the MW path on the ROHF surface for $H_2CO^{-\bullet} + CH_3Cl$ (a) near the TS, (b) in the flat, intermediate region, and (c) in the ET product valley.

is the C−C coordinate which makes the difference. It collapses in the SUB(C) case to an quilibrium C−C bond, while recoiling and dephasing the bonding in the ET case. The unusual feature of the $OH_2C\cdots CH_3\cdots Cl^-$ transition state, which distinguishes it from a classical transition state for a SUB process, is illustrated in Figure 7 which shows the reaction vector at the transition state and along the MW path of the ROHF level, obtained from reaction path-following on the full 21-dimensional potential energy surface. As seen from the displacement vectors in Figure 7a, the two hydrogen substituents of the formaldehyde flap against the methyl group in opposition to the C−C approach. Thus, when the flat region of the potential energy surface is reached, the C−C bond does not change as much but the C−Cl bond lengthens more rapidly (Figure 7b). Subsequently, in Figure 7c, the $H_2C{=}O$ moiety recoils and both the C−C and C−Cl bonds lengthen as the path descends into the ET valley. Thus, the hydrogen flapping mode is associated with the inhibition of C−C bond making past the TS and loss of bonding en route to the dissociated ET products.[7] The flapping mode of the formyl hydrogens is found also in the ET-TS of the $Cl(CH_2)_3C(H)O^{-\bullet}$ system (**4c** in Scheme 2). Animation of the mode in the latter system shows that the flapping hydrogen acts like a tennis racket and hits the $CH_2\cdots Cl$ moiety whenever the CH_2 carbon approaches the formyl carbon.

The flapping motion represents, in fact, a chemically simple[18] *mechanism by which bonded ET-TS lose its C−C bonding*. Thus, since the carbonyl group undergoes pyramidalization by C−C bonding in the TS (see, e.g., structure **4b** in Scheme 2), the flapping mode serves simply to restore the planarity of the carbonyl as required by the structure of the ET product. While, there may exist a variety of recoil mechanisms for bonded ET-TS, the hydrogen flapping mode in the reaction vector appears as an indicator of ET character.

The $OH_2C\cdots CH_3\cdots Cl^-$ transition state on the UHF surface exhibits the same reaction vector as the ROHF ET-TS in Figure 7a. In fact, at all levels employed for the $H_2C{=}O^{-\bullet} + CH_3Cl$ reaction, one obtains the same vector,[7] indicating the unique feature of this TS that is essentially a bonded ET-TS, albeit it may lead to both the ET and the SUB(C) products owing to the broad ridge separating the valleys.

Path-Following Behavior for Bonded ET-TS. This is an appropriate place to emphasize some common features which are expected for the path-following of bonded-ET reactions and of borderline situations. All these systems will have two valleys separated by a ridge, which can in turn be high or low. The C···C···X (e.g., X = Cl) type ET-TS will be located at the onset of the ET valley which follows toward the dissociated ET product limit. The ridge will be located at shorter C−C distances than the ET-TS, while the ET valley will lie at longer C−C distances relative to the ridge.

Starting from the ET-TS, the Z-Int path will trace the ET valley, and the recoil of the C···C distance will occur quite early along the path (see Figure 5). The MW path will behave in a different manner because light particles move farther than heavy particles (i.e., CH_3 in **4b** or the central CH_2 in the intramolecular cases, **4c** and **4d**). This movement will shorten the C···C distance, and as such, the MW path will initially head toward the ridge. Because of this property of the MW path, it is expected to exhibit an imaginary projected frequency. Such *imaginary frequencies are however indications of the ridge character of the MW path*, with no mechanistic significance otherwise. What matters is the overall behavior of the MW path, which depends on the height of the ridge. Whenever this ridge is high enough, the MW path will bounce back to the ET valley and head toward the dissociated ET products. In these cases, the mechanistic assignments of the Z-Int and MW paths will be identical and unequivocal, as found here for the **4b** (in ROHF) and for **4c** and **4d**. The main difference between the paths will be the later C···C recoil in the MW path compared with that in the Z-Int path (see Figure 5b). An opposite mechanistic assignment of the Z-Int and MW paths will occur whenever the ridge is sufficiently broad to be crossed by the MW path. Such findings may serve therefore as an indication for a potential surface branching (e.g., **4b** in UHF) where the ET-TS may slide through the ET valley, or may enter the flat ridge region and bifurcate thereafter to the ET and SUB(C) products.

A Valence Bond (VB) Analysis of the Reaction Pathways for the ET-SUB(C) Competition. The foregoing discussion projects four isostructural TS with partial C−C bonding: one for $H(CN)C{=}O^{-\bullet} + CH_3Cl$ which leads to SUB(C), two for $Cl(CH_2)_3C(H)O^{-\bullet}$ and $Cl(CH_2)_2C(H)O^{-\bullet}$ which lead to ET, and one for $H_2C{=}O^{-\bullet} + CH_3Cl$ which may qualify as a borderline situation leading to both mechanisms. This pattern as well as much of what has been described in earlier papers[2,7] can be understood by appreciating that the electronic structure of the bonded ET-TS cannot be described by two electronic configurations as in the traditional theory of outersphere electron transfer.[1−3,7,8e,j,19]

The principal VB configurations which need to be considered are shown in Figure 8, using the main orbitals of the ketyl anion radical and methyl chloride reactants, π_{CO}, π^*_{CO}, σ_{CX}, and σ^*_{CX}. In the Φ_{ET} configuration, the electron has been transferred from π^*_{CO} to σ^*_{CX}. In the $\Phi_{SUB(C)}$ configuration, the formyl moiety is in a triplet arrangement; the three odd electrons are paired into an overall doublet spin and involve an electron pair which becomes the C−C bond in the SUB(C) product.[7] At the geometry of the reactants, the energy difference between the ET and SUB(C) configuration is given by the triplet excitation of the formyl unit ($\pi_{CO} \rightarrow \pi^*_{CO}$).

(18) The same type of flapping mode was found in the ET-TS of $H_2S + C_2H_6^{+\bullet}$. No such mode was found in the corresponding SUB-TS for the same reactants. See: Cho, J. K.; Shaik, S. S. *J. Am. Chem. Soc.* **1991**, *113*, 9890.

(19) Reddy, A. C.; Danovich, D.; Ioffe, A.; Shaik, S. *J. Chem. Soc., Perkin Trans. 2* **1995**, 1525.

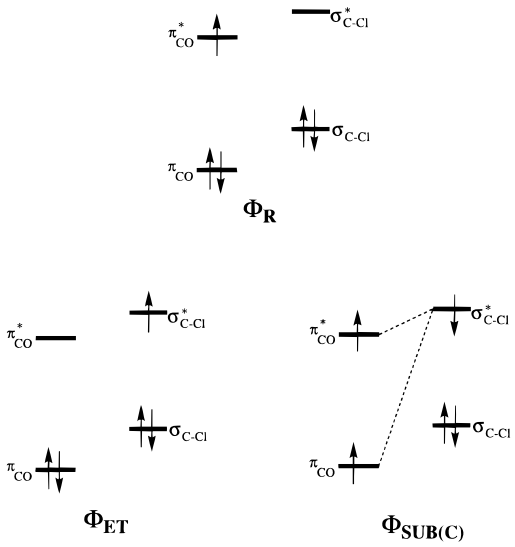

Figure 8. VB configurations for discussion of the ET and SUB(C) reaction mechanisms for $H_2CO^{-\bullet}$ + CH_3Cl, $Cl(CH_2)_nC(H)O^{-\bullet}$ (n = 2, 3) and $H(CN)CO^{-\bullet}$ + CH_3Cl.

The pairwise avoided crossing of these three configurations gives rise to the three potential TS for the ketyl anion radical/methyl chloride system. The avoided crossing of Φ_R and Φ_{ET} leads to an ET transition state which is stabilized by partial C−C bonding, while the avoided crossing of Φ_R and $\Phi_{SUB(C)}$ leads to a SUB(C) transition state. The third avoided crossing, between Φ_{ET} and $\Phi_{SUB(C)}$, results in the TS for the radical attack process (see R_{AT}-TS in Figure 1 and 3). The ridge between the SUB(C) and ET channels is also affected by these avoided crossing mechanisms. Thus, for example, for an ET mechanism the ridge, which exists in a cross-section of smaller C−C distances, will be determined initially by the Φ_R and $\Phi_{SUB(C)}$ avoided crossing and further at shorter C−C distances by the avoided crossing between Φ_{ET} and $\Phi_{SUB(C)}$. We may expect therefore that the potential energy surfaces of this family of reactions will be similar, whereas the height of the ridge and the depth of the valleys will depend on the avoided crossing situations typical to each case.

The two avoided crossings important for the present problem are between Φ_R and Φ_{ET} and between Φ_R and $\Phi_{SUB(C)}$. The mechanistic question (ET or SUB(C)) for a given reactant pair may be reduced to the question of whether Φ_{ET} or $\Phi_{SUB(C)}$ is first to cross the reactant configuration, Φ_R, along the C−C−Cl trajectory. As long as the triplet excitation of the formyl unit ($\pi_{CO} \rightarrow \pi^*_{CO}$) is large, Φ_{ET} lies well below $\Phi_{SUB(C)}$ and the first crossing along the C−C−Cl trajectory will be between Φ_{ET} and Φ_R. The secondary mixing of $\Phi_{SUB(C)}$ into the Φ_R-Φ_{ET} avoided crossing state will lead to an ET-TS which possesses significant C−C bonding. Movement from the ET-TS along the same trajectory, to shorter C−C distances, will encounter the $\Phi_{SUB(C)}$-Φ_R avoided crossing. Consequently, the ET-TS will be accompanied by a ridge at shorter C−C distances and a second valley that leads to SUB(C) products. The height of the ridge will be determined by the relative stability of the ET and SUB(C) products; the more stable the SUB(C) product is, the lower the ridge, and vice versa. This situation fits the reactions of $Cl(CH_2)_nC(H)O^{-\bullet}$ and $H_2C{=}O^{-\bullet}$ with CH_3Cl. In these cases, the triplet energy of formaldehyde[20] is >5 eV, and hence, the Φ_{ET} and $\Phi_{SUB(C)}$ configurations are well separated in energy; the avoided crossing will be dominated by Φ_R-Φ_{ET} with a smaller mixing of the $\Phi_{SUB(C)}$ configuration. For $Cl(CH_2)_3C(H)O^{-\bullet}$ and $Cl(CH_2)_2C(H)O^{-\bullet}$ where the SUB(C) product is less stable than the ET product due to the strain of the small rings in the SUB(C) product, the ridge will be significant and the transition state will be an ET transition state exclusively. In contrast, for the $H_2C{=}O^{-\bullet}$ with CH_3Cl reaction, where the SUB(C) product is significantly more stable (Figure 3), the ridge separating the ET-like TS and the SUB(C) valley will be low and can be crossed easily. *Thus, while a trajectory nascent from the ET-TS may still remain in the ET valley, it can also enter the flat ridge region and bifurcate thereafter to the ET and SUB(C) products.*

Unless inhibited by structural constraints like those in the intramolecular cases, the $\Phi_{SUB(C)}$ configuration descends more steeply along the C−C−Cl trajectory than Φ_{ET}. Thus, when the formaldehyde derivative possesses a low triplet excitation energy, and when the SUB(C) reaction is exothermic while the ET process is endothermic or very weakly exothermic, the first avoided crossing along the C···C···Cl trajectory is between $\Phi_{SUB(C)}$ and Φ_R. This is the situation for $H(CN)CO^{\bullet-}/CH_3Cl$ reactant pair (Figure 1), where the ET process is slightly endothermic and where the triplet energy of the cyanoformaldehyde is reduced to <3 eV. The $\Phi_{SUB(C)}$-Φ_R avoided crossing leads to a SUB(C)-TS, as in Figure 1. This SUB(C)-TS will have a small ET character due to the secondary mixing of Φ_{ET} into the TS, while at longer C−C distances there will be a ridge due to the Φ_R-Φ_{ET} avoided crossing.

The foregoing VB analysis shows that the bonded-ET and the SUB(C) mechanisms are entangled, and a series of reactants is likely to exhibit a mechanistic changeover from ET to SUB(C) with borderline situations, as shown in the present study.

Conclusions

Ketyl radical anions + CH_3Cl (CH_3X in general) and $Cl(CH_2)_nC(H)O^{-\bullet}$ undergo two types of reactions that have isostructural transition states (Scheme 1). One reaction is substitution at carbon, SUB(C), and the other is dissociative electron transfer, ET. From the TS for $H(CN)CO^{-\bullet}$ + CH_3Cl, **4a** in Figure 1, the reaction path (with or without mass weighting) proceeds to the SUB(C) products. Thus, the $H(CN)CO^{-\bullet}$ + CH_3Cl system exhibits a SUB(C) mechanism which results in C-alkylation products. In contrast, the reactions of $Cl(CH_2)_nC(H)O^{-\bullet}$ leads to ET products via a bonded-ET-TS, irrespective of the path-following method (**4c** and **4d** in Figure 2). The corollary of these results with experimental systems[5] is noted, and as such, *bonded ET-TS which obey orbital selection rules[1] and possess definite stereochemistry should be regarded as viable alternatives to the weakly bonded outer sphere TS.*

For the reaction of $H_2CO^{-\bullet}$ with CH_3Cl (**4b** in Figure 3), the steepest descent path using Z-matrix internal coordinates proceeds to dissociated ET products on both the UHF and ROHF surfaces. However, using mass-weighted coordinates, the path heads initially on to the ridge; with UHF, it descends to SUB(C) products, and with ROHF, it leads to ET products. The potential energy surface descends from the transition state to a broad, flat region that branches into two valleys. Under such circumstances, small differences in the coordinate system and level of theory can lead to different results. Calculations at higher level of theory (UQCISD(T)/6-31G*) tentatively suggest that the ridge separating the TS from the SUB(C) valley is broad. In such a case, a trajectory nascent from the ET-TS may slide through the ET valley, or may enter the flat ridge region and

(20) The triplet energy of formaldehyde is approximately 5 eV. See: (a) Merchan, M.; Roos, B. O. *Theor. Chim. Acta* **1995**, *92*, 227. (b) Buenker, B. J.; Peyrimhoff, S. D. *J. Chem. Phys.* **1970**, *53*, 2368.

bifurcate thereafter to the ET and SUB(C) products. The topology of these potential energy surfaces can lead to interesting dynamic consequences which are beyond the scope of the present investigation.

A VB analysis allows some understanding of the origins of the ET-SUB(C) mechanistic competition and the difficulties associated with the mechanistic characterization by computational means. The ET and SUB(C) mechanisms are shown to be entangled because their constituent VB configurations mix along the common section of the C···C···Cl trajectory. Thus, a case is made here for isostructural TS which obey orbital selection rules,[1] possess partial C−C bonding, lead to ET, SUB(C), and borderline mechanisms. Even though the experimental findings for ketyl radical anions and alkyl halide favor ET reactivity over a SUB(C) mechanism,[5,8g−i] the notion of an ET-TS which can bifurcate also to SUB(C) is still worthy of further exploration.

Acknowledgment. *This paper is dedicated to Lennart Eberson on the occasion of his 65th birthday*. The research at HU is sponsored in part by the Volkswagen Stiftung and in part by a grant from The Israel Science Foundation. The work at WSU is supported by the National Science Foundation (CHE 94-00678).

Supporting Information Available: Z-Matrix structures of the transition states and valley ridge inflection points (4 pages). See any current masthead page for ordering and Internet access instructions.

JA971105D